AJNR

Correlation of Quantitative Diffusion Tensor Tractography with Clinical Grades of Subacute Sclerosing Panencephalitis

R. Trivedi, H. Anuradha, A. Agarwal, R.K.S. Rathore, K.N. Prasad, R.P. Tripathi and R.K. Gupta

AJNR Am J Neuroradiol 2011, 32 (4) 714-720
doi: https://doi.org/10.3174/ajnr.A2380
http://www.ajnr.org/content/32/4/714

ORIGINAL RESEARCH

R. Trivedi
H. Anuradha
A. Agarwal
R.K.S. Rathore
K.N. Prasad
R.P. Tripathi
R.K. Gupta

Correlation of Quantitative Diffusion Tensor Tractography with Clinical Grades of Subacute Sclerosing Panencephalitis

BACKGROUND AND PURPOSE: SSPE is a persistent infection of the central nervous system caused by the measles virus. The correlation between the clinical staging and conventional MR imaging is usually poor. The purpose of this study was to determine whether tract-specific DTI measures in the major white mater tracts correlate with clinical grades as defined by the Jabbour classification for SSPE.

MATERIALS AND METHODS: Quantitative DTT was performed on 20 patients with SSPE (mean age, 9 years) and 14 age- and sex-matched controls. All patients were graded on the basis of the Jabbour classification into grade II ($n = 9$), grade III ($n = 6$), and grade IV ($n = 5$) SSPE. The major white matter tracts quantified included the CC, SLF, ILF, CST, CNG, SCP, MCP, ICP, ATR, STR, and PTR.

RESULTS: Although a successive decrease in mean FA values was observed in all the fiber tracts except for the SCP and ICP, moving from controls to grade IV, a significant inverse correlation between clinical grade and mean FA values was observed only in the splenium ($r = -0.908$, $P < .001$), CST ($r = -0.663$, $P = .013$), SLF ($r = -0.533$, $P = .050$), ILF ($r = -0.776$, $P = .001$), STR ($r = -0.538$, $P = .047$), and PTR ($r = -0.686$, $P = .035$) fibers. No significant correlation of mean MD values from these white matter tracts was observed with clinical grades of the disease.

CONCLUSIONS: We conclude that the grade of encephalopathy correlates inversely with the tract-specific mean FA values. This information may be valuable in studying the disease progression with time and in assessing the therapeutic response in the future.

ABBREVIATIONS: ATR = anterior thalamic radiations; CC = corpus callosum CC1 = rostrum; CC2 = genu; CC3 = rostral body; CC4 = anterior midbody; CC5 = posterior midbody; CC6 = isthmus; CC7 = splenium; CNG = cingulum; CST = corticospinal tracts; DTI = diffusion tensor imaging; DTT = diffusion tensor tractography; EEG = electroencephalography; FA = fractional anisotropy; FLAIR = fluid-attenuated inversion recovery; ICP = inferior cerebellar peduncle; ILF = inferior longitudinal fasciculus; MCP = middle cerebellar peduncle; MD = mean diffusivity; *P* = *P* value; PTR = posterior thalamic radiations; *R* = correlation; SCP = superior cerebellar peduncle; SFM = stable fiber mass; SLF = superior longitudinal fasciculus; SSPE = subacute sclerosing panencephalitis; STR = superior thalamic radiations

SSPE is a rare and fatal complication of the common measles virus infection, especially in children. Symptoms of SSPE usually appear after a latent period of approximately 6–8 years of clinical infection,[1] and SSPE results in death within 2–4 years of its onset.[2,3] The 5 diagnostic criteria of SSPE include clinical presentation, characteristic EEG findings, abnormal CSF findings, high measles antibody titers in serum and CSF, and positive findings on brain biopsy.[4] A diagnosis of SSPE can be reliably established if the patient fulfills 3 of the 5 criteria. Typically, early symptoms of SSPE involve regressive changes in intellect and personality. Usually mental disturbances are followed by myoclonus, convulsions, and abnormal postures; progressing to optic atrophy, motor weakness, and akinetic mutism; and ending in coma and death.[3]

Received July 12, 2010; accepted after revision September 7.

From the Departments of Radiodiagnosis (R.T., R.K.G.) and Microbiology (K.N.P.), Sanjay Gandhi Post Graduate Institute of Medical Sciences, Lucknow, India; Nuclear Magnetic Resonance Research Centre (R.T., R.P.T.), Institute of Nuclear Medicine and Allied Sciences, Delhi, India; Department of Neurology (H.A., A.A.), Chhatrapati Shahuji Maharaj Medical University, Lucknow, India; and Department of Mathematics and Statistics (R.K.S.R.), Indian Institute of Technology, Kanpur, India.

Please address correspondence to R.K. Gupta, MD, MR Section, Department of Radiodiagnosis, Sanjay Gandhi Post Graduate Institute of Medical Sciences, Lucknow, India-226014; e-mail: rgupta@sgpgi.ac.in, rakeshree1@gmail.com

DOI 10.3174/ajnr.A2380

Conventional MR imaging findings poorly correlate with the clinical grade of the disease.[5,6] A recent voxel-based morphometric study has reported reduced cortical gray matter volume in the frontotemporal regions of patients with SSPE; however, no correlation was observed between the gray matter distribution and neurologic disability index scores or the duration of symptoms in these patients.[7] Metabolite abnormalities in the normal-appearing white matter of patients with SSPE have been described on in vivo proton MR spectroscopy.[1,8] Aydin et al[9] have shown significant correlation between clinical severity and absolute concentration of *N*-acetylaspartate and myo-inositol in the frontal white matter of patients with SSPE. Diffusion-weighted imaging studies have reported increased apparent diffusion coefficient values in normal-appearing white matter on MR imaging in patients with SSPE compared with controls.[1,10-12]

DTI, an extension of the diffusion imaging technique, has been shown to be valuable in studies of neuroanatomy, compact white matter fiber connectivity, and brain development. A region of interest–based morphometric DTI study has shown abnormal FA values in the parieto-occipital white matter and splenium, even in the patients with grade II SSPE with normal conventional imaging findings.[13] The popular region of interest–based morphometric DTI method is not always

reliable because of the uncertainty of manual specification and its limitation to 2D, which does not reflect the whole fiber bundle in 3D space. In brain white matter, the principal diffusion direction corresponds well with the orientation of major fibers in each voxel. DTT offers an overall view of individual fiber bundles in 3D spaces.[14] In addition to basic 3D visualization, many studies have used fiber tracking to delineate specific white matter tracts for quantitative analysis. Quantitative DTT studies have examined the microstructure of white matter tracts in healthy control subjects[15-20] as well as in patients with various neuropathologies.[21,22]

We hypothesized that microstructural damage in white matter tracts in various grades of SSPE could be detected by using quantitative DTT. The purpose of this study was to verify the above-mentioned hypothesis by demonstrating the probable correlation between tract-specific DTI metrics in major white matter pathways and Jabbour classification, based on clinical grades of SSPE.[23]

Materials and Methods

We examined 20 children (16 boys and 4 girls) with SSPE (mean age, 9 years). All patients were consistently right-handed. The diagnosis of SSPE was based on a typical clinical presentation, EEG pattern, and elevated CSF antimeasles antibody titer.[23] In all these cases, the characteristic EEG pattern was suppression burst episodes, in which high-amplitude slow and sharp waves of 3–5 seconds recur at intervals of 5–8 seconds on a slow background. For the detection and titration of antibodies to the measles virus, a passive particulate agglutination test (Serodia-Measle; Fujirebio, Tokyo, Japan) was performed. CSF antibody titer $\geq$ 1:128 was considered positive for measles virus infection. The age at which measles infection occurred ranged from 6 months to 2 years in all children. There was a mean latent period of 8 years (range, 4–11 years) for the onset of clinical symptoms in patients with a history of measles. There was a mean gap of 5 months (range, 2–12 months) between the onset of symptoms and the imaging in all these patients.

We used Jabbour classification[23] for the clinical staging and found that of 20 children, 9 were in grade II, 6 were in grade III, and 5 were in grade IV SSPE. Most children had such cognitive decline that they could not give information beyond their names or identify simple objects like a pen or watch. Detailed neuropsychological evaluation could not be performed in these patients.

We also performed MR imaging on 14 right-handed age- and sex-matched healthy controls (age range, 5–12 years; 8 boys and 6 girls) to compare age-related changes in brain parenchyma in children with SSPE. None of the controls had any neurologic disease and were not on any medication. The institutional research ethics committee approved the study. Informed consent was obtained from the parents of patients and controls for the MR imaging examination.

MR Imaging Protocol

MR imaging was performed on a 1.5T MR imaging system (Signa; GE Healthcare, Milwaukee, Wisconsin) equipped with an actively shielded whole-body magnetic field gradient set with a maximal strength of 33 mT/m and a quadrature birdcage receive-and-transmit radio-frequency head coil. The conventional MR imaging protocol included a T2-weighted fast spin-echo sequence with TR/TE/echo-train length/NEX, 6000/200 ms/16/2; a T1-weighted spin-echo sequence with TR/TE/NEX, 800/14 ms/1; and a FLAIR sequence with TR/TE/TI, 9000/89/2200 ms. Postcontrast T1-weighted imaging was performed after injecting 0.1 mmol/L/kg body weight of gadodiamide (Omniscan; Amersham Health, Oslo, Norway) intravenously. DTI data were acquired by using a single-shot echo-planar dual spin-echo sequence with ramp sampling. The diffusion-weighting b factor was set to 1000 s/mm^2, TR $\sim$ 8 seconds, TE $\sim$ 100 ms, and NEX = 8. The diffusion tensor encoding used was a dodecahedral scheme with 10 uniformly distributed directions. All imaging was performed in the axial plane and had identical geometric parameters: FOV, 240 $\times$ 240 mm^2; section thickness, 3 mm; and section gap, 0. Segmentation of white matter structures and DTT was performed by using in-house-developed JAVA-based software.[19]

Segmentation of White Matter Structures

The key idea of this method is to segment the principal eigenvector field into stable voxels having a minimal e^1 variation (curvature).[19] Thus, a voxel P (i, j, k) is a member of the SFM, if there is a neighboring voxel Q (x, y, z) such that the principal eigenvectors e^1s at P and Q point to each other. Mathematically, it translates to the relation G [F (P)] = P, where F (P) = ROUND (P + e^1(P) + 0.5u), u = (1,1,1), and G (Q) = ROUND (Q − e^1(Q) + 0.5u); the function ROUND stands for the component-wise "integral part" operation.

The method first generates a SFM and then segments the volume by coloring the voxel P according to the values the components (l, m, n) of the vector joining P and Q take: ($\pm$1,0,0) red, (0,$\pm$1,0) green, (0,0,$\pm$1) blue, ($\pm$1,$\pm$1,0) yellow, (0,$\pm$1,$\pm$1) cyan, ($\pm$1,0,$\pm$1) magenta, and ($\pm$1,$\pm$1,$\pm$1) white. A nonstable voxel is gray, and a voxel with FA $<$ 0.15 remains black. Typical segmented axial, sagittal, and coronal SFM color maps are generated; this method narrows down the region-of-interest selection for the standard tractography to pointing out a color segment inside a broader region of interest through a single mouse click.[19]

DTT

Different fiber bundles have characteristic signature segments (Fig 1) on the SFM color maps and are automatically and reproducibly reconstructed by providing these segments as regions of interest to the fiber assignment by a continuous-tracking algorithm.[24] This reconstruction allowed us to identify the coordinates of specific white matter tracts and to investigate the anatomy. DTI measures were calculated for the entire fiber. An FA threshold of 0.15 was used for fiber tracking.

Data Quantitation

Major white matter fiber tracts, including the CC, SLF, ILF, CST, CNG, SCP, MCP, ICP, ATR, STR, and PTR, were generated and quantified by using in-house–developed JAVA-based software (Fig 1).

Details of the generation of the white matter fiber tracts (SLF, ILF, CNG) are described in detail elsewhere.[19] The CC fibers were further divided into 7 segments (ie, the rostrum, genu, rostral body, anterior midbody, posterior midbody, isthmus, and splenium) by using the scheme proposed by Witelson[25] in a manner that approximately represents the CC connections hypothesized across cortical brain regions.[26] For the reconstruction of ATR, MCP, SCP, and ICP, the mouse clicks were made on the coronal SFM color map segments where the thickness of the respective fiber bundle was at a maximum (Fig 1). In the case of CST, STR, and PTR, the same procedure was adopted by using the axial SFM color map segments associated with these structures (Fig 1).

Statistical Analysis

A Student paired *t* test was performed to evaluate the differences between DTI measures in all the white matter tracts of the right hemisphere and those of the left hemisphere in healthy controls. Multiple

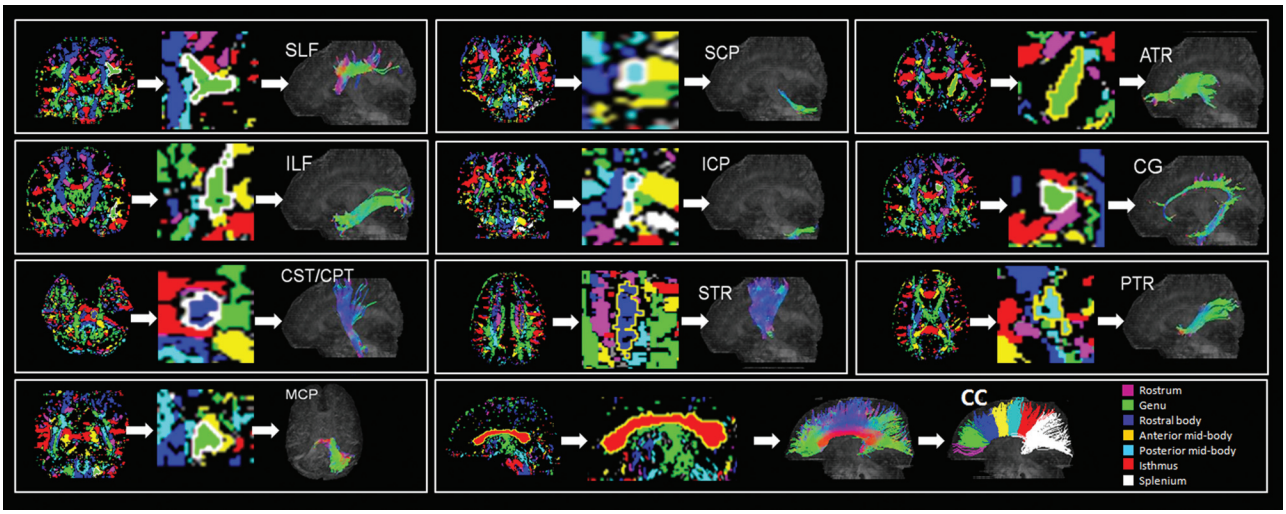

Fig 1. Demonstration of the methodology used for white matter tract reconstruction from a 9-year-old healthy subject. Red, green, and blue represent left-to-right, anterior-to-posterior, and superior-to-inferior directions, respectively.

comparisons by using the Bonferroni post hoc test were performed to determine the changes in FA and MD values among controls and clinical grades of patient groups. Bivariate analysis of correlation was performed to study the relationship between the white mater tract−specific DTI measures and the clinical grade of SSPE, with the assumption that there was no correlation between DTI measures and clinical grade (Ho = null hypothesis). Alternatively, if a correlation of <0.001 was observed at $\alpha = 0.05\%$ and 90% power of the test, the null hypothesis was rejected. A P value $\leq .05$ was considered to be significant. All statistical analyses were performed by using the Statistical Package for the Social Sciences software, Version 15.0 (SPSS, Chicago, Illinois).

Results

Qualitative Analysis

On conventional MR imaging, 12 of the 20 patients showed qualitative abnormalities. In children with grade II SSPE, 5 had normal findings and 4 showed abnormal signal intensities in brain parenchyma on conventional imaging. Six children had SSPE with grade III; of them, 1 had normal findings and 5 showed abnormal findings on conventional imaging. In the remaining 5 of 20 children with grade IV, 3 showed abnormal imaging findings and 2 had normal findings on conventional imaging. Lesions were hyperintense on T2-weighted/FLAIR images and iso- to hypointense on T1-weighted images and were distributed in the periventricular and/or subcortical white matter. In the remaining 8 patients, no abnormalities were detected on conventional MR imaging.

In patients, lesions were distributed in the centrum semiovale ($n = 7$), frontal white matter ($n = 7$), parieto-occipital white matter ($n = 9$), temporal white matter ($n = 5$), splenium ($n = 2$), and thalamus ($n = 1$). There was no abnormal parenchymal or meningeal enhancement on postcontrast T1-weighted imaging in any of the patients.

Quantitative Analysis

There was no significant change in the mean FA and MD values in the white matter fiber tracts of the right cerebral hemisphere compared with the left hemisphere in controls, indicating the absence of any significant cerebral lateralization. For the purpose of quantitative analysis, DTI measures collected from the right and left hemispheres in all of the white matter tracts (except the CC) were pooled together. The mean ± SD of FA and MD values of various fiber bundles in controls and patients of different grades are summarized in Table 1.

Comparative Analysis of FA

A successive decrease in mean FA values was observed in the whole CC as well as in all of the 7 segments of the CC, moving from controls to grade IV through grades II and III (Fig 2). In the entire CC, significantly decreased mean FA values in all patient groups were observed compared with controls. Within the patient groups, in the whole CC and splenium, a significant decrease in mean FA values was observed, moving from controls to grade IV through grades II and III. In genu, rostral body, anterior midbody, and isthmus, patients with grade IV showed significantly decreased mean FA values compared with those with grade II. However, no significant difference was observed between patients with grades II and III or between those with grades III and IV. In the genu and posterior midbody, no significant difference was observed among patient groups.

In addition to the CC, a successive decrease in mean FA values was observed in all white matter tracts except for the SCP and ICP, moving from controls to grade IV through grades II and III (Fig 2). Among all the white matter tracts quantified in our study, significantly decreased FA values in patient groups were observed in the CST, SLF, ILF, ATR, STR, and PTR compared with controls. Among the patient groups, significantly decreased mean FA in grade IV was observed compared with grade II in the ILF and CNG.

Comparative Analysis of MD

Although the MD values in entire CC of all patient groups were increased compared with those of controls, they did not reach the significance level. Successive increases in MD values were observed only in the ILF, moving from controls to grade IV through grades II and III.

Table 1: Summary of group means and SDs of the FA and MD from the white matter tracts of brain collected from the age- and sex-matched controls and patients with SSPE of different clinical grades

Fiber Bundles	FA				MD ($\times 10^{-3}$ mm^2/s)			
	Controls	Grade II	Grade III	Grade IV	Controls	Grade II	Grade III	Grade IV
CC1	0.34 ± 0.02	0.29 ± 0.02	0.28 ± 0.02	0.27 ± 0.05	0.82 ± 0.04	0.81 ± 0.04	0.87 ± 0.13	0.85 ± 0.05
CC2	0.38 ± 0.01	0.33 ± 0.04	0.30 ± 0.03	0.27 ± 0.04	0.81 ± 0.01	0.85 ± 0.10	0.85 ± 0.08	0.88 ± 0.15
CC3	0.35 ± 0.02	0.30 ± 0.02	0.28 ± 0.02	0.24 ± 0.04	0.81 ± 0.04	0.91 ± 0.13	0.82 ± 0.05	0.99 ± 0.39
CC4	0.36 ± 0.02	0.31 ± 0.02	0.30 ± 0.02	0.25 ± 0.04	0.82 ± 0.05	0.87 ± 0.09	0.86 ± 0.14	0.95 ± 0.12
CC5	0.35 ± 0.02	0.31 ± 0.03	0.30 ± 0.03	0.26 ± 0.04	0.83 ± 0.06	0.86 ± 0.10	0.87 ± 0.11	0.86 ± 0.15
CC6	0.36 ± 0.02	0.30 ± 0.03	0.26 ± 0.03	0.24 ± 0.02	0.84 ± 0.06	0.85 ± 0.11	0.81 ± 0.04	0.88 ± 0.08
CC7	0.40 ± 0.02	0.34 ± 0.02	0.29 ± 0.01	0.25 ± 0.02	0.85 ± 0.07	0.86 ± 0.09	0.85 ± 0.07	0.87 ± 0.11
SLF	0.30 ± 0.01	0.25 ± 0.02	0.24 ± 0.02	0.22 ± 0.03	0.75 ± 0.02	0.81 ± 0.14	0.76 ± 0.10	0.76 ± 0.09
ILF	0.34 ± 0.02	0.30 ± 0.02	0.27 ± 0.02	0.25 ± 0.02	0.66 ± 0.07	0.78 ± 0.11	0.76 ± 0.08	0.81 ± 0.07
CNG	0.29 ± 0.02	0.26 ± 0.03	0.24 ± 0.01	0.22 ± 0.02	0.79 ± 0.06	0.94 ± 0.16	1.00 ± 0.26	0.79 ± 0.10
MCP	0.41 ± 0.02	0.37 ± 0.03	0.37 ± 0.04	0.35 ± 0.03	0.79 ± 0.11	0.77 ± 0.12	0.72 ± 0.04	0.76 ± 0.13
SCP	0.35 ± 0.01	0.32 ± 0.02	0.33 ± 0.03	0.32 ± 0.02	0.85 ± 0.14	0.97 ± 0.22	0.86 ± 0.10	0.81 ± 0.09
ICP	0.35 ± 0.02	0.33 ± 0.03	0.31 ± 0.03	0.32 ± 0.02	0.79 ± 0.06	0.92 ± 0.18	0.82 ± 0.07	0.77 ± 0.06
CST	0.33 ± 0.01	0.28 ± 0.02	0.27 ± 0.02	0.25 ± 0.01	0.73 ± 0.02	0.78 ± 0.12	0.78 ± 0.08	0.79 ± 0.10
ATR	0.30 ± 0.01	0.27 ± 0.03	0.26 ± 0.01	0.25 ± 0.02	0.77 ± 0.03	0.90 ± 0.26	0.75 ± 0.11	0.80 ± 0.11
STR	0.31 ± 0.01	0.27 ± 0.03	0.26 ± 0.02	0.23 ± 0.03	0.76 ± 0.03	0.88 ± 0.20	0.78 ± 0.09	0.96 ± 0.53
PTR	0.35 ± 0.02	0.31 ± 0.02	0.29 ± 0.02	0.28 ± 0.03	0.80 ± 0.08	0.92 ± 0.14	0.86 ± 0.13	0.75 ± 0.10

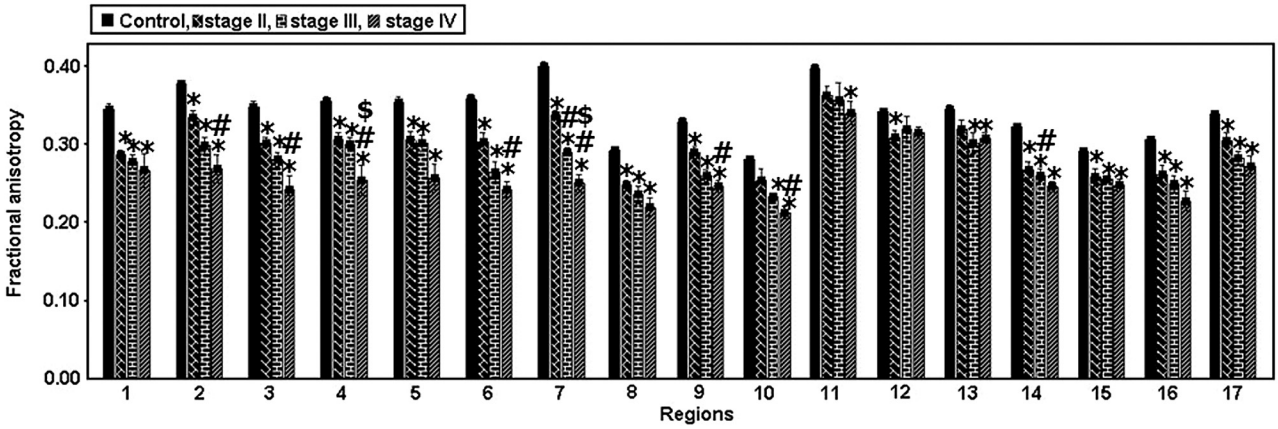

Fig 2. Plot showing the FA values of 7 segments of the CC and other major white matter tracts of patients with different grades of SSPE and age- and sex-matched healthy controls: 1) rostrum, 2) genu; 3) rostral body, 4) anterior midbody, 5) posterior midbody, 6) isthmus, 7) splenium, 8) SLF, 9) ILF, 10) CNG, 11) MCP, 12) SCP, 13) ICP, 14) CST, 15) ATR, 16) STR, 17) PTR. Asterisks denote a significant difference between control and patient groups; the number sign, a significant difference in patients with grade II from grades III and IV; and the dollar sign, a significant difference between patients with SSPE of grades III and IV.

Table 2: Summary of the correlations between clinical grade and DTI measures (FA and MD) of whole fiber bundles of CC in patients with SSPE

Grade	Rostrum	Genu	Rostral Body	Anterior Midbody	Posterior Midbody	Isthmus	Splenium	Whole CC
FA								
R	−0.276	−0.690	−0.687	−0.571	−0.507	−0.681	−0.908	−0.811
P	.252	.001	.001	.011	.027	.001	<.001	<.001
MD								
R	0.277	0.113	0.113	0.140	0.014	0.117	0.044	0.112
P	.251	.645	.646	.566	.955	.632	.860	.648

Correlation between DTI Measures and Clinical Grade

Significant inverse correlation of clinical grades with mean FA values was observed in all segments of the CC (except the rostrum) (Table 2). Among other major white matter fibers, a significantly inverse correlation between mean FA values and clinical grades was observed in the CST, SLF, ILF, STR, and PTR (Table 3).

In all the white matter tracts, no significant correlation was observed between MD values and clinical grades (Tables 2 and 3).

Discussion

To the best of our knowledge, this is the first quantitative DTT study showing major white matter tracts in children with SSPE and their comparison with age- and sex-matched controls. This study demonstrates the correlation between clinical grades and DTI measures in major white matter tracts in children with SSPE.

In this study, 8 patients showed normal imaging findings, even though they shared similar clinical profiles with children who had abnormal findings on conventional imaging. These

Table 3: Summary of the correlations between clinical grade and DTI measures (FA and MD) of whole fiber bundles of major white matter tracts (except CC) in patients with SSPE

Grade	CST	SLF	ILF	CNG	MCP	SCP	ICP	ATR	STR	PTR
FA										
R	−0.663	−0.533	−0.776	−0.648	−0.295	0.134	−0.226	−0.268	−0.538	−0.686
P	.013	.050	.001	.117	.305	.648	.437	.355	.047	.035
MD										
R	0.504	−0.205	0.157	−0.374	−0.020	−0.442	−0.494	−0.257	0.104	0.525
P	.093	.481	.593	.208	.946	.114	.073	.375	.723	.066

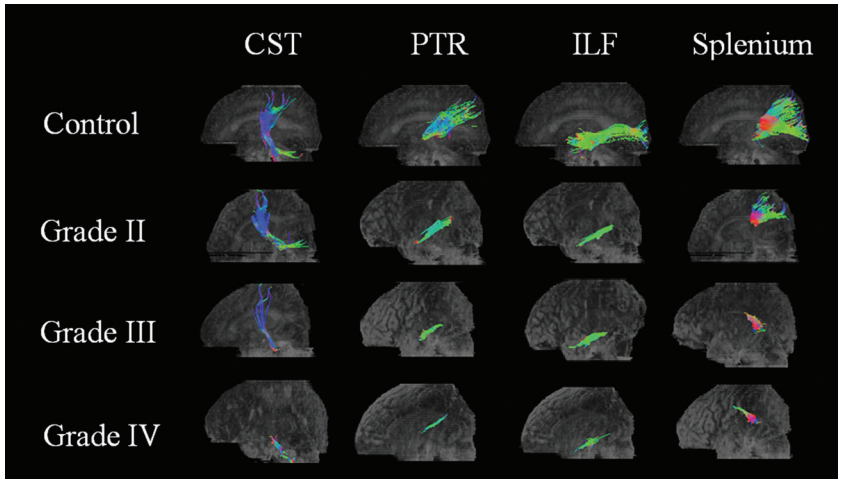

Fig 3. Projection of the CST, PTR, ILF, and splenium on the midsagittal plane in subject groups shows a subsequent decrease in fiber tracts, moving from controls to patients with SSPE grade IV through grades II and III.

data suggest that conventional MR imaging is inadequate for the assessment of clinical grade. It is well-documented that the severity of conventional MR imaging changes correlate poorly with the clinical findings.[5,6] Patients with severe disease may still have normal findings on conventional MR imaging examinations.[9] On a single-voxel proton MR spectroscopic study, Aydin et al[9] have shown a significant correlation between clinical severity and *N*-acetylaspartate and myo-inositol in the frontal white matter of patients with SSPE. However, the localized spectroscopic approach does not reflect the degree of damage in the entire brain. In contrast to conventional MR imaging, mean FA values in major white matter tracts were found to be abnormal in all patients, even in those who had normal MR imaging findings. Our observations of abnormal DTI measures in patients with SSPE can be explained by pathologic changes, like astrogliosis, neuronal loss and degeneration, demyelination, neurofibrillary tangles, and infiltration of inflammatory cells.[27-30] Significant inverse correlation of mean FA with clinical grades suggests that FA is a better measure than conventional MR imaging for the assessment of clinical grade in these patients.

In the present study, we observed reduced mean FA in major white matter tracts of patients with SSPE compared with healthy controls. Similar results have been obtained on previous DTI studies in patients with grade II SSPE, which showed significantly reduced FA values with increased MD values in the CC as well as periventricular white matter.[13] Pathologically, mild inflammation of the cortical gray matter is prominent in the early stage of the disease; which progresses to subcortical and deep white matter involvement.[31] In the later phase of the disease, the inflammation subsides, leading to demyelination, necrosis, and gliosis.[28] The posterior regions, especially the parieto-occipital and posterotemporal areas, are predominantly affected early in the course of the disease.[32] The conventional MR imaging findings usually appear normal in the early stages, with sequential involvement of posterior parts of the cerebral hemisphere as the disease progresses.[31] With time, high-signal-intensity changes in the deep white matter and severe cerebral atrophy occur on T2-weighted images.[31]

On bivariate correlation analysis, a significant inverse correlation of clinical grade was observed with mean FA values quantitated from whole tracts of the CC (all segments of the CC except the rostrum), SLF, ILF, CST, STR, and PTR. The CC is associated with different aspects of human behavior, cognition, and normal aging.[33] Cognitive decline is the common clinical feature in patients with SSPE.[3] In this study, FA values in the patient groups were significantly reduced in all segments of the CC (except the rostrum) compared with those in healthy controls, suggestive of microstructural damage in the interhemispheric fibers from the hemispheric lobes that pass from the different segments of the CC. Periventricular white matter abnormality is a common feature in SSPE. Previous MR imaging studies[13,34] have reported the involvement of the CC and have explained its involvement secondary to periventricular white matter abnormality. Among all major white matter tracts quantified in this study, the correlation of FA with clinical grade was much stronger in the splenium than in other white matter tracts (Fig 3). In a histopathologic study, de Lacoste et al[26] reported that white matter fibers from the parieto-occipital junctional region course through the splenium of the CC. The predominant involvement of the parieto-oc-

cipital region during the course of the disease is probably responsible for a stronger correlation between mean splenial FA and clinical grade.

In this study, strong significant inverse correlations between FA and clinical grade were observed in CC followed by CST, ILF, and PTR (Table 3 and Fig 3). Pyramidal signs and symptoms usually develop in higher grades of SSPE.[28] Motor impairments have been attributed to the injury of CST fibers. A DTI study in patients with SSPE has indicated significantly decreased FA in the posterior limb of the internal capsule in patients with SSPE compared with healthy controls, even in the absence of motor dysfunction.[13] The authors speculated that decreased FA in the absence of motor dysfunction is an early indicator of structural abnormality of the motor fibers in SSPE. Our study confirms the above-mentioned postulation by demonstrating a significant inverse correlation between FA values collected from the CST and clinical grade. The ILF connects the extrastriate occipital cortex with the lateral temporal cortex, parahippocampal gyrus, and amygdala, while the PTR establish connections between the thalamus and cortex of the occipital lobe. A much stronger correlation of FA with clinical grade in the splenium, ILF, and PTR compared with other white matter tracts can be explained on the basis of preferential involvement of the parieto-occipital region of the brain during disease progression.[3,13]

A relatively weak correlation between FA and clinical grade was observed in the SLF and STR. The SLF is located at the superolateral side of the putamen and forms an arc, sending branches to the frontal, parietal, occipital, and temporal lobes[19]; and the STR connects the ventralis posteromedialis and ventralis posterolateralis nuclei to the postcentral gyrus (parietal lobe). They contain reciprocal parietothalamic fibers and corticothalamic fibers for other thalamic nuclei. We speculate that the small contribution of the fibers emerging from the parieto-occipital lobe to the SLF and STR is probably responsible for the weak inverse correlation of FA with clinical grade in these tracts.

MD reflects change in cell attenuation and extracellular space.[35] Increased MD values in all white matter pathways of the patients with SSPE compared with controls could be attributed to increased extracellular water content because of marked gliosis and microscopic/macroscopic cystic changes in the brain parenchyma of patients with SSPE. Although the MD values in patients was high compared with controls in all white matter tracts, no consecutive change in MD values was observed in moving from controls to grade IV. Decreased FA with no change in MD has been found in various pathologic conditions.[13,36] An increased FA in the first 24 hours after trauma with no change in MD has also been reported.[37] DTI studies in brain abscess have shown large variation in FA values, with no significant changes in MD values.[38,39] The observations from previous studies suggest that FA does not have a relationship with MD. The significant inverse correlation of mean FA with clinical grades suggests that FA is a better measure than MD for the assessment of clinical grades in these patients. The lack of a correlation between MD values in white matter tracts and clinical grades may also be attributed to the small number of patients in grades III and IV.

The limitations of the current study are the smaller number of patients in different clinical grades and the lack of long-term follow-up. Grade I SSPE is subtle and is usually noticed by declining school performance or behavior changes. Usually the children with grade II SSPE report to clinics. Although the unavailability of children with grade I SSPE is another limitation of this study, quantification of DTT-derived metrics helped in reducing the discrepancy between imaging and clinical findings. Demonstration of involvement of the fibers connected to the parieto-occipital brain on DTT, especially in patients with normal findings on conventional imaging, may be used as an early sign of SSPE in young children with a history of childhood fever, skin rashes, and poor school performance along with behavior changes.

Conclusions

We conclude that the grade of encephalopathy correlates inversely with the tract-specific mean FA value. This information may be valuable in studying the disease progression with time and in assessing the therapeutic response to therapy in the future.

References

1. Alkan A, Sarac K, Kutlu R, et al. **Early- and late-state subacute sclerosing panencephalitis: chemical shift imaging and single-voxel MR spectroscopy.** *AJNR Am J Neuroradiol* 2003;24:501–06
2. Graves MC. **Subacute sclerosing panencephalitis.** *Neurol Clin* 1984;2:267–80
3. Garg RK. **Subacute sclerosing panencephalitis.** *Postgrad Med J* 2002;78:63–70
4. Dyken PR. **Subacute sclerosing panencephalitis: current status.** *Neurol Clin* 1985;3:179–96
5. Brismar J, Gascon GG, Steyern KV, et al. **Subacute sclerosing panencephalitis: evaluation with CT and MR.** *AJNR Am J Neuroradiol* 1996;17:761–72
6. Oztürk A, Gürses C, Baykan B, et al. **Subacute sclerosing panencephalitis: clinical and magnetic resonance imaging evaluation of 36 patients.** *J Child Neurol* 2002;17:25–29
7. Aydin K, Okur O, Tatli B, et al. **Reduced gray matter volume in the frontotemporal cortex of patients with early subacute sclerosing panencephalitis.** *AJNR Am J Neuroradiol* 2009;30:271–75
8. Cakmakci H, Kurul S, Iscan A, et al. **Proton magnetic resonance spectroscopy in three subacute sclerosing panencephalitis patients: correlation with clinical status.** *Childs Nerv Syst* 2004;20:216–20
9. Aydin K, Tatli B, Ozkan M, et al. **Quantification of neurometabolites in subacute sclerosing panencephalitis by 1H-MRS.** *Neurology* 2006;67:911–13
10. Alkan A, Korkmaz L, Sigirci A, et al. **Subacute sclerosing panencephalitis: relationship between clinical stage and diffusion-weighted imaging findings.** *J Magn Reson Imaging* 2006;23:267–72
11. Sener RN. **Subacute sclerosing panencephalitis findings at MR imaging, diffusion MR imaging, and proton MR spectroscopy.** *AJNR Am J Neuroradiol* 2004;25:892–94
12. Oksuzler YF, Cakmakci H, Kurul S, et al. **Diagnostic value of diffusion-weighted magnetic resonance imaging in pediatric cerebral diseases.** *Pediatr Neurol* 2005;32:325–33
13. Trivedi R, Gupta RK, Agarawal A, et al. **Assessment of white matter damage in subacute sclerosing panencephalitis using quantitative diffusion tensor MR imaging.** *AJNR Am J Neuroradiol* 2006;27:1712–16
14. Mukherjee P, Chung SW, Berman JI, et al. **Diffusion tensor MR imaging and fiber tractography: technical considerations.** *AJNR Am J Neuroradiol* 2008;29:843–52
15. Partridge SC, Mukherjee P, Berman JI, et al. **Tractography-based quantitation of diffusion tensor imaging parameters in white matter tracts of preterm newborns.** *J Magn Reson Imaging* 2005;22:467–74
16. Lebel C, Walker L, Leemans A, et al. **Microstructural maturation of the human brain from childhood to adulthood.** *Neuroimage* 2008;40:1044–55
17. Eluvathingal TJ, Hasan KM, Kramer L, et al. **Quantitative diffusion tensor tractography of association and projection fibers in normally developing children and adolescents.** *Cereb Cortex* 2007;17:2760–68
18. Giorgio A, Watkins KE, Douaud G, et al. **Changes in white matter microstructure during adolescence.** *Neuroimage* 2008;39:52–61
19. Trivedi R, Agarwal S, Rathore RK, et al. **Understanding development and lateralization of major cerebral fiber bundles in pediatric population through quantitative diffusion tensor tractography.** *Pediatr Res* 2009;66:636–41
20. Hasan KM, Iftikhar A, Kamali A, et al. **Development and aging of the healthy human brain uncinate fasciculus across the lifespan using diffusion tensor tractography.** *Brain Res* 2009;1276:67–76

21. Catani M. **Diffusion tensor magnetic resonance imaging tractography in cognitive disorders.** *Curr Opin Neurol* 2006;19:599–606
22. Trivedi R, Agarwal S, Shah V, et al. **Correlation of quantitative sensorimotor tractography with clinical grade of cerebral palsy**. *Neuroradiology* 2010;52:759–65. Epub 2010 Apr 20
23. Jabbour JT, Garcia JH, Lemmi H, et al. **Subacute sclerosing panencephalitis: a multidisciplinary study of eight cases.** *JAMA* 1969;207:2248–54
24. Mori S, Crain BJ, Chacko VP, et al. **Three-dimensional tracking of axonal projections in the brain by magnetic resonance imaging.** *Ann Neurol* 1999;45:265–69
25. Witelson SF. **Hand and sex differences in the isthmus and genu of the human corpus callosum: a postmortem morphological study.** *Brain* 1989;112:799–835
26. de Lacoste MC, Kirkpatrick JB, Ross ED. **Topography of the human corpus callosum.** *J Neuropathol Exp Neurol* 1985;44:578–91
27. Parker JC, Klintworth GK, Graham DG, et al. **Uncommon morphologic features in subacute sclerosing panencephalitis (SSPE).** *Am J Pathol* 1970;61:275–92
28. Ohya T, Martinez AJ, Jabbour JT, et al. **Subacute sclerosing panencephalitis: correlation of clinical, neurophysiologic, and neuropathologic findings.** *Neurology* 1974;24:211–18
29. Mandybur TI. **The distribution of Alzheimer's neurofibrillary tangles and gliosis in chronic subacute sclerosing panencephalitis.** *Acta Neuropathol* 1990;80:307–10
30. Poon TP, Tchertkoff V, Win H. **Subacute measles encephalitis with AIDS diagnosed by fine needle aspiration biopsy: a case report.** *Acta Cytol* 1998;42:729–33
31. Tuncay R, Akman-Demir G, Gökyigit A, et al. **MRI in subacute sclerosing panencephalitis**. *Neuroradiology* 1996;38:636–40
32. Kulezycki J, Kryst-Widzgowska T, Sobczyck W, et al. **NMR and CT images in subacute sclerosing panencephalitis.** *Neurol Neurochir Pol* 1994;28:79–90
33. Abe O, Aoki S, Hayashi N, et al. **Normal aging in the central nervous system: quantitative MR diffusion-tensor analysis.** *Neurobiol Aging* 2002;23:433–41
34. Anlar B, Saatçi I, Köse G, et al. **MRI findings in subacute sclerosing panencephalitis.** *Neurology* 1996;47:1278–83
35. Rugg-Gunn FJ, Symms MR, Barker GJ, et al. **Diffusion imaging shows abnormalities after blunt head trauma when conventional magnetic resonance imaging is normal.** *J Neurol Neurosurg Psychiatry* 2001;70:530–33
36. Gupta RK, Saksena S, Agarwal A, et al. **Diffusion tensor imaging in late posttraumatic epilepsy.** *Epilepsia* 2005;46:1465–71
37. Field AS, Hasan K, Jellison BJ, et al. **Diffusion tensor imaging in an infant with traumatic brain swelling.** *AJNR Am J Neuroradiol* 2003;24:1461–64
38. Gupta RK, Hasan KM, Mishra AM, et al. **High fractional anisotropy in brain abscesses versus other cystic intracranial lesions.** *AJNR Am J Neuroradiol* 2005;26:1107–14
39. Gupta RK, Nath K, Prasad A, et al. **In vivo demonstration of neuroinflammatory molecule expression in brain abscess with diffusion tensor imaging.** *AJNR Am J Neuroradiol* 2008;29:326–32